RESEARCH ARTICLE SUMMARY

ARCHAIC HOMININS

Long-term isolation and archaic introgression shape functional genetic variation in Near Oceania

Patrick F. Reilly, Stephen Rong, Daniela Tejada-Martinez, Samantha L. Miller, Audrey Tjahjadi, Chang Liu, Jared Akers, Alysa Pomer, Margaret E. Prentice, D. Andrew Merriwether, Françoise R. Friedlaender, George Koki, Jonathan S. Friedlaender, Steven K. Reilly, Serena Tucci*

Full article and list of author affiliations: https://doi.org/10.1126/science.adr6749

INTRODUCTION: Because of their different settlement histories, the Pacific Islands have been divided into Near and Remote Oceania. Near Oceania—the region consisting of New Guinea, the Bismarck Archipelago, and the main Solomon Islands—was settled ~42,000 years ago and thereafter remained largely isolated at the edge of human settlement. Not until ~5000 years ago, with the advent of new migration pressures from Asia, were the rest of the Pacific Islands inhabited—Remote Oceania, encompassing Vanuatu, New Caledonia, Fiji, Polynesia, and Micronesia. Near Oceanic populations harbor substantial cultural, phenotypic, and genetic diversity, including the largest amounts of archaic introgression inherited from Neanderthals and Denisovans. However, they have been substantially underrepresented in whole-genome sequencing and functional genomic consortia to date.

RATIONALE: We sequenced 177 high-coverage genomes from 12 diverse Near Oceanic populations and analyzed them alongside 1284 genomes from worldwide populations. We investigated the demographic history of groups descended from early settlers of the Pacific and the extent and distribution of Neanderthal and Denisovan introgression in Near Oceanic genomes, including adaptive archaic variation, and performed a massively parallel reporter assay to identify the functional consequences of adaptive archaic introgressed variants.

RESULTS: Near Oceanians in our study fall along a gradient of genetic similarity from Papuan-speaking groups of New Guinea and the Baining of New Britain to the Polynesian outlier groups of the Solomon Islands, although we also observed signals of long-term isolation in Papuan-speaking groups. Furthermore, both the Baining and Polynesian outlier groups showed evidence of major population bottlenecks, emphasizing complex population structure and demographic history in this region. We reconstructed archaic introgressed sequence covering 70.7% of the callable archaic genome (1.897 billion base pairs) including 505 million base pairs (Mbp) of previously unidentified archaic sequence and three times more Denisovan sequence than previous studies (831.9 Mbp). We uncovered evidence for introgression from three Denisovan-like groups into the ancestors of Near Oceanians, revealing a new twist on our interactions with archaic hominins. We refined maps of archaic "deserts" and identified a strong novel signal of adaptive Denisovan introgression at *TRPS1*, a skeletal development gene previously found under selection in central African rainforest hunter-gatherers and highland Ecuadorians. Using a massively parallel reporter assay, we discovered 3127 high-frequency introgressed expression-modulating variants targeting 1422 genes and found an enrichment of high-frequency introgressed variants with protein-coding, splicing, and regulatory impacts on immune pathways. These include adaptive archaic variants affecting genes in the interferon-γ pathway, including *JAK1*, *GBP2*, and the COVID-19–associated *OAS1* locus, where we functionally characterized a Denisovan haplotype unique to Oceanic populations. Although some of these adaptive introgression signals, such as *TNFAIP3* and *HLA-DRA*, may be related to malaria susceptibility, few are widely shared across Near Oceania, suggesting multiple independent instances of local adaptation. Many of these immune-related genes are also pleiotropic, including *TRPS1* and *TANK*.

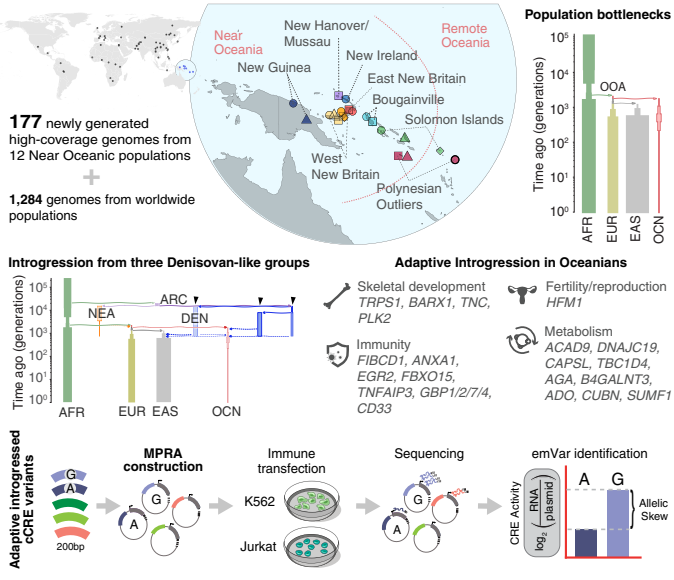

The complex evolutionary history of Near Oceanians. Map of Oceanic and other worldwide populations included in this study, along with models showing a strong bottleneck (narrow population bar) and three Denisovan introgression events (dashed arrows) into Oceanians, targets of adaptive introgression in Oceanians, and a diagram of the method used to detect functional effects of archaic variants. AFR, Africans; OOA, Out-of-Africa; EUR, Europeans; EAS, East Asians; OCN, Oceanians; NEA, Neanderthals; DEN, Denisovans; ARC, archaic hominins; cCRE, candidate cis-regulatory element; MPRA, massively parallel reporter assay; emVar, expression-modulating variant.

CONCLUSION: We characterized the evolutionary, phenotypic, and functional consequences of archaic introgressed variants in Near Oceanians and identified putatively causal archaic variants contributing to parallel local adaptation of both the immune system and skeletal development. □

*Corresponding author. Email: serena.tucci@yale.edu Cite this article as P. F. Reilly *et al.*, *Science* **392**, eadr6749 (2026). DOI: 10.1126/science.adr6749

ARCHAIC HOMININS

Long-term isolation and archaic introgression shape functional genetic variation in Near Oceania

Patrick F. Reilly[1], Stephen Rong[2], Daniela Tejada-Martinez[1]†, Samantha L. Miller[1], Audrey Tjahjadi[1], Chang Liu[1], Jared Akers[2], Alysa Pomer[1]‡, Margaret E. Prentice[2], D. Andrew Merriwether[3], Françoise R. Friedlaender[4]§, George Koki[5], Jonathan S. Friedlaender[4], Steven K. Reilly[2], Serena Tucci[1,6]*

Near Oceanic populations harbor substantial cultural, phenotypic, and genetic diversity yet are drastically underrepresented in human genomics. We generated 177 high-coverage Near Oceanian whole genomes and analyzed them alongside 1284 worldwide genomes, revealing major distinctions among and within islands, including long-term isolation and strong population bottlenecks. We reconstructed 1.897 billion base pairs of the archaic genome, including 831.9 million base pairs of Denisovan sequence, and found evidence for introgression from three Denisovan-like groups in Near Oceanians and adaptive Denisovan introgression at *TRPS1*, a skeletal development gene also under selection in central African rainforest hunter-gatherers and highland Ecuadorians. We then performed a massively parallel reporter assay and discovered 3127 high-frequency introgressed expression-modulating variants, finding an enrichment of functional impacts on genes in the interferon-γ signaling pathway including *JAK1*, *GBP2*, and *OAS1*.

Near Oceania—the region consisting of New Guinea, the Bismarck Archipelago, and the main Solomon Islands (*1*)—was inhabited by at least 42,000 years ago (*2*), and present-day humans in this region harbor substantial genetic and phenotypic diversity (*3*, *4*), including the largest amounts of archaic hominin introgression (*5*). However, Near Oceanic populations are substantially underrepresented in modern whole-genome sequencing and functional genomic consortia (*6*–*9*). To fill one of the largest gaps in representation, we sequenced and analyzed a large, geographically and linguistically diverse sample of Near Oceanic individuals and leveraged these data to understand the evolutionary, functional, and phenotypic consequences of underrepresented human genetic variation.

Long-term isolation and bottlenecks strongly structure genetic variation in Near Oceania

We sequenced the genomes of 177 individuals from 12 geographically and linguistically diverse populations across Near Oceania to a median depth of 31.6×. These genomes were jointly called and analyzed along with published genomes, for a total of 1221 unrelated individuals from 79 worldwide populations (Fig. 1A) (*5*, *6*, *10*–*12*). Across this dataset, we identified 61,471,552 single nucleotide variants (SNVs) and 4,792,088 short insertion-deletion variants (indels) (figs. S1 to S11 and tables S1 to S3) (*13*). By comparing the proportion of shared, known, and novel region-private SNVs among major geographic regions, we found that Oceanic groups harbor the largest proportion of region-private SNVs outside of Africa (~44.1%), of which ~48.2% were previously unidentified (Fig. 1B and figs. S12 and S13).

Genetic drift leads to the accumulation of differences in allele frequencies between groups, which can be exacerbated by long-term isolation and bottleneck events. Applying principal components analysis (PCA) and ADMIXTURE, we observed a gradient of genetic similarity in worldwide groups from Africans to Near Oceanic individuals as well as substantial genetic drift of the Baining-Kagat and Baining-Mali, two inland groups of East New Britain (figs. S14 to S17). Focusing on a regional level, Oceanic populations fall along another gradient of genetic similarity from the Polynesian outlier groups of the Solomons (Bellona, Rennell, and Tikopia) at one extreme to Papuan-speaking groups of New Guinea (Sepik and Goroka) and the Bismarck Archipelago (Baining-Kagat, Baining-Mali) at the other (Fig. 1C). Signals of genetic drift were observed in these Papuan-speaking groups [including Ata and Mamusi (*14*)] as well as the Polynesian outlier groups (Fig. 1, C and D, and figs. S14 to S21). These patterns of population structure are further supported by fixation index (F_{ST}) and outgroup f_3 analyses (figs. S18, S19, and S22). Other groups along this admixture gradient appear equally divergent from New Guinean and Baining groups, suggesting symmetric divergence from an ancestral Near Oceanic population (figs. S23 to S26 and table S4). These results are broadly consistent with the scenario of an extended period of isolation of >15,000 years following the initial Pleistocene settlement of Near Oceania, as well as a much later population movement ultimately linked to Taiwan (*15*) associated with the expansion of Austronesian-speaking peoples as early as ~3300 years ago (*16*). The interplay between this admixture gradient and structure within the inland/Papuan-speaking and Polynesian outlier clusters leads to five main ancestry components corresponding to the New Guinean groups, the Baining groups, the Ata and Mamusi, Bougainvilleans, and the Polynesian outlier groups (Fig. 1D and fig. S21), suggesting potential bottlenecks in the historical population sizes of these groups (*17*).

We next examined patterns of long runs of homozygosity (ROH) and inferred effective population size histories using SMC++ (*18*). Large amounts of long ROH may arise from a recent strong bottleneck, a prolonged bottleneck, or both. Accordingly, the Baining-Mali, Baining-Kagat, and Bellona/Rennell had the largest genome-wide proportion of ROH in Oceania (F_{ROH} = 9.9, 8.3, and 12.5%, respectively; Fig. 1E and figs. S27 to S29) and an excess of long [4 to 16 million base pairs (Mbp)] and very long (>16 Mbp) ROH relative to other Oceanic groups in our sample (figs. S30 and S31). Inferred effective population size curves indicate two main patterns that could explain these ROH results: A strong bottleneck between 10 and 20 thousand years ago (kya), and a distinct signal of blunted population growth around 30 kya (Fig. 1F and figs. S32 to S34). The latter signal was identified exclusively in the Baining-Mali and Bellona/Rennell, whereas the former was strongest in the Baining-Kagat and Tikopia (~85 to 90% reductions in effective population size), and weaker in the Ata, Mamusi, Kove, Goroka, and Taiwanese Atayal. In concert with a previous demographic reconstruction of a small Baining sample (*19*), these results provide strong evidence for long-term isolation and a geographically restricted deep bottleneck in an ancestral Near Oceanic population preceding the Austronesian expansion.

Archaic hominin introgression in Near Oceania

Although DNA introgressed from Neanderthals can be found in all modern humans outside of Africa, Denisovan introgression is primarily found in Oceanic individuals (figs. S35 to S44) (*20*). To detect genomic regions introgressed from archaic hominins, we applied the reference-free approach implemented in Sprime (*21*) to 1120 geographically diverse

[1]Department of Anthropology, Yale University, New Haven, CT, USA. [2]Department of Genetics, Yale School of Medicine, New Haven, CT, USA. [3]Department of Anthropology, Binghamton University, Binghamton, NY, USA. [4]Department of Anthropology, Temple University, Philadelphia, PA, USA. [5]Papua New Guinea Institute for Medical Research, Goroka, East Highlands Province, Papua New Guinea. [6]Department of Ecology and Evolutionary Biology, Yale University, New Haven, CT, USA. ***Corresponding author. Email: serena.tucci@yale.edu** †Present address: Weinberg ALS Center, Vickie and Jack Farber Institute for Neuroscience, Department of Neuroscience, Thomas Jefferson University, Philadelphia, PA, USA. ‡Present address: Center for Surgery and Public Health, Brigham and Women's Hospital, Boston, MA, USA. §Deceased.

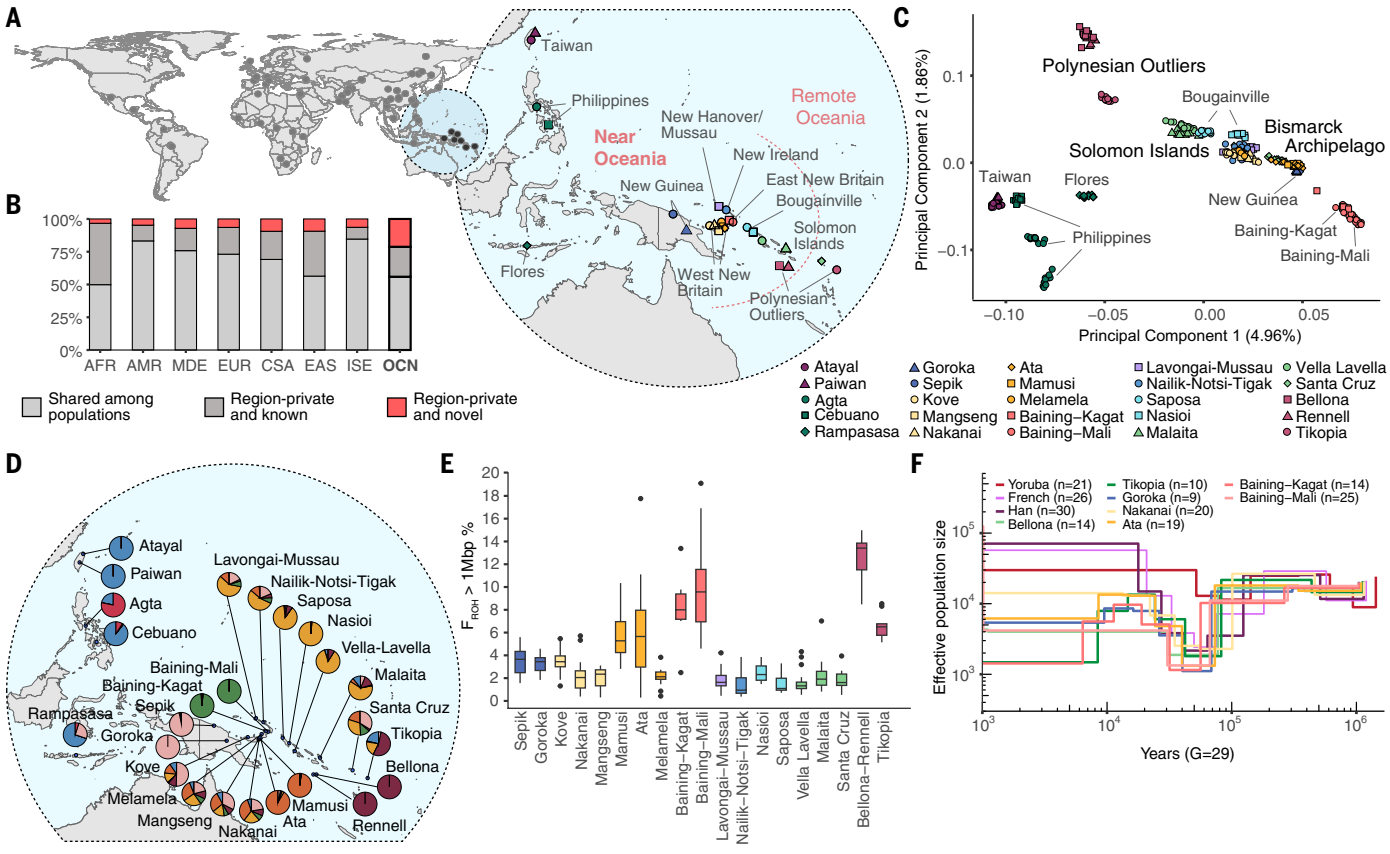

Fig. 1. Sampling locations, novel variants, and population structure in Oceania. (**A**) Locations of 79 worldwide populations studied. Inset shows populations in Taiwan, Island Southeast Asia, and Oceania, including 177 newly sequenced Near Oceanic individuals from 12 diverse populations across New Britain, New Hanover, New Ireland, and Bougainville. (**B**) Proportion of shared, known, and novel region-private SNVs among populations in major geographic regions. Novel variants are SNVs absent from dbSNP build 154 and published genomic datasets (the 1000 Genomes Project phase 3 call set, and gnomAD release 2.1.1 exomes and genomes) (*13*). For abbreviations, see table S1. (**C**) PCA of Oceanic, Taiwanese, and Island Southeast Asian individuals. (**D**) ADMIXTURE analysis. The proportion of each component in each pie chart is calculated as the mean across individuals for each ancestral cluster per population for $K = 7$. (**E**) Per-sample genome-wide proportion of runs of homozygosity (F_{ROH}) in Oceanic populations. (**F**) Historical effective population sizes for selected worldwide and Oceanic populations inferred with SMC++. The *x* axis is scaled from generations into years on the basis of 29 years per generation. Diploid sample size used for each population is indicated by the n value in parentheses.

human genomes from outside of Africa, including 146 unrelated, newly generated Near Oceanic genomes (*13*). We determined the archaic origin of each tract on the basis of its match rate to the published Altai Denisovan and three Neanderthal genomes (figs. S45 to S47). We found that Oceanic genomes carry ~2.5-fold more archaic introgressed sequence from all origins per individual than European genomes (median 141.2 versus 56.2 Mbp; Fig. 2A, fig. S48, and table S5) and 14-fold more Denisovan sequence per individual than East Asian genomes (median 36.1 versus 2.5 Mbp; Fig. 2A and table S6).

Introgressed sequence can be combined across individuals to reconstruct archaic genomes; the amount of the archaic genome reconstructed in this manner is called "archaic coverage." The introgressed sequence we recovered from all origins spanned 70.7% of the callable genome [1.897 billion base pairs (Gbp)], more than a quarter of which is previously undocumented (505.2 Mbp; Fig. 2B) (*5*, *13*, *22*). This includes almost threefold more Denisovan sequence than previously identified (831.9 Mbp) (*5*, *23*), most of which was found in Oceanic samples (591.1 Mbp; table S7), highlighting the importance of Oceanic genomes to expanding the catalog of introgressed archaic hominin variants. Large gaps in these genomic maps of archaic introgression (called "archaic deserts") may provide evidence for strong purifying selection against archaic variants (*5*, *22*, *23*). We identified 166 archaic deserts (gaps ≥ 1 Mbp) spanning ~11% of the callable genome (292.7 Mbp; table S8). These regions showed strong signals of background selection compared with the rest of the genome (Cliff's delta: 0.288 to 0.369; fig. S49) and were significantly enriched in constrained genes compared with archaic introgressed regions [odds ratio (OR) = 1.59, 95% confidence interval = [1.27, 1.98], $P = 3.2 \times 10^{-5}$, fitness reduction for heterozygous loss-of-function (LoF) carriers (s_{het}) top versus bottom 10%], consistent with purifying selection on archaic introgression, although hybrid incompatibilities may also have contributed (*23*). Among five previously identified deserts (≥10 Mbp) (*5*, *23*), four were more finely resolved by archaic introgressed tracts in our dataset (fig. S50). Of the 155 genes previously thought to reside in these large archaic deserts, 15 overlap newly defined archaic introgressed regions (table S9). The remaining 140 included salivary and pancreatic amylase genes thought to have undergone a selective sweep in the modern human lineage after divergence from Neanderthals and Denisovans (*24*, *25*).

Within Oceania, levels of introgression were highly heterogeneous, varying by almost twofold from the New Guinean Sepik and Goroka groups (median 180.8 and 176.9 Mbp) to New Britain's Nakanai and the Polynesian outlier groups of Bellona and Rennell (median 98.2 and 99.7 Mbp; Fig. 2A and table S5). We found that Sepik individuals harbored the most Denisovan introgression, 25 times more than East Asians (median 60.0 versus. 2.5 Mbp, ~1.1% versus ~0.05%; Fig. 2A and table S6). In line with prior work (*11*, *12*, *19*, *26*, *27*), we found that the

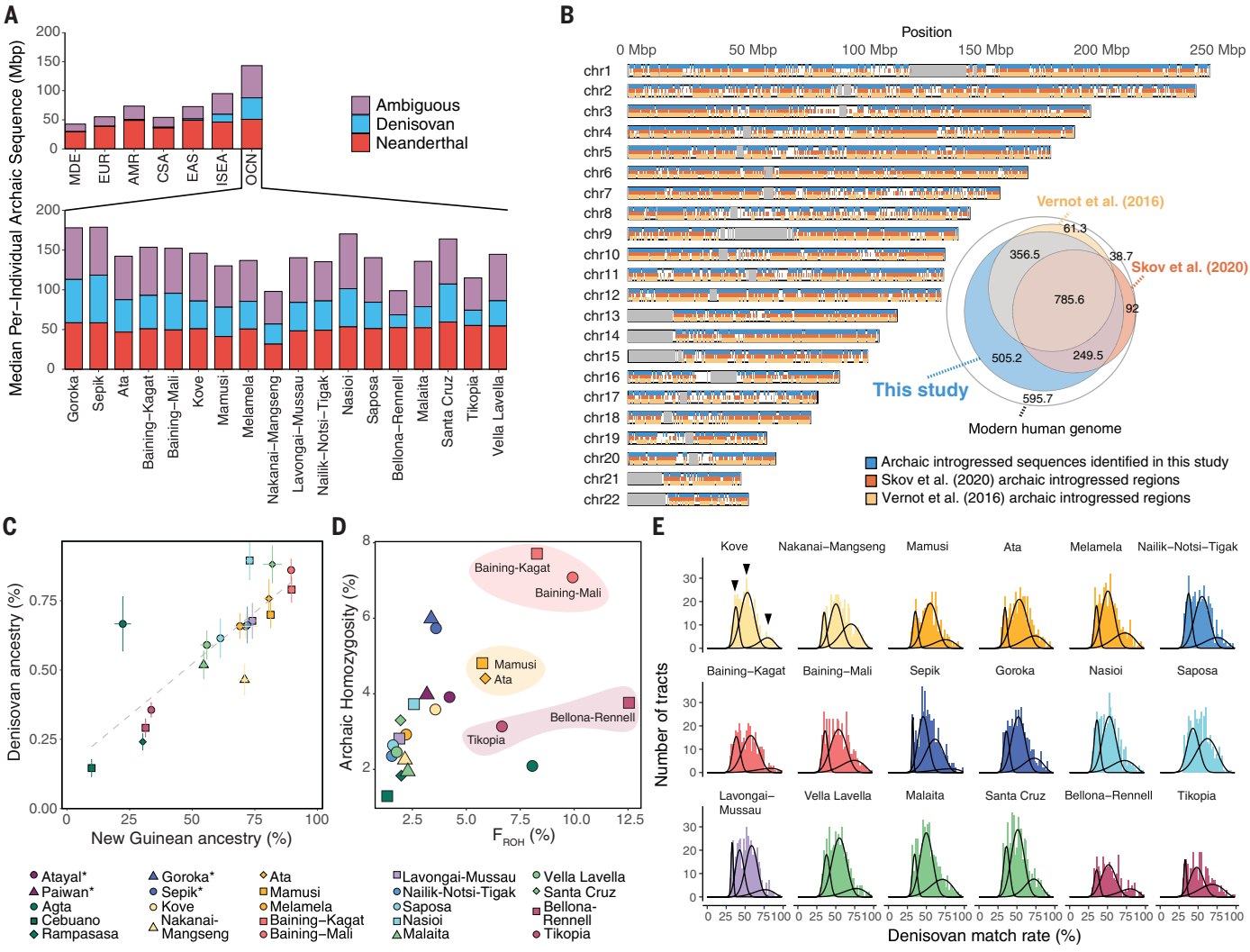

Fig. 2. Archaic hominin introgression in present-day Oceanic genomes. (**A**) Median amounts of Neanderthal, Denisovan, and ambiguous introgressed sequence in millions of base pairs (Mbp) per individual in each major geographic region (top) and each Oceanic population (bottom). (**B**) Genomic distribution of archaic introgressed regions identified in this study (blue), Skov *et al*. (*22*) (red), and Vernot *et al*. (*5*) (yellow). Masked genomic regions are shown in gray. Euler diagrams show the amount of overlap in total archaic sequence (in Mbp) identified in the three studies, where the largest circle represents the callable modern human genome (autosomes minus masked regions). (**C**) Per-population average proportion of Denisovan introgression identified using Sprime (*y* axis) compared with average proportion of New Guinean ancestry inferred by RFMix (*x* axis). Bars indicate ±1 standard deviation about the mean. The regression (gray dashed line) for groups outside the Bismarck Archipelago is shown for reference. Asterisks in the legend denote populations omitted owing to being used in the local ancestry inference reference panel for calculating New Guinean ancestry. (**D**) Per-population average percentage of sites in archaic introgressed tracts that are homozygous for the putative archaic allele (*y* axis) as compared with per-population average F_{ROH} as a percentage (*x* axis). (**E**) Beta mixture model fits (black curves) of the match rates to the Altai Denisovan genome of Denisovan introgressed tracts identified in Oceanic populations.

genomic proportion of Denisovan introgression in Island Southeast Asian and Near Oceanic groups increased with greater shared ancestry with New Guineans, with the Philippine Agta as the sole exception ($\beta = 0.70\%$, $P < 2.2 \times 10^{-16}$; Fig. 2C and figs. S51 and S52).

Comparing per-individual levels of introgression with archaic coverage can provide insights into differences in admixture and demographic history between populations (*28*). We found that despite harboring 41% more Neanderthal introgression per individual and having ~45% larger sample size in our dataset, Oceanic genomes had 28% less Neanderthal coverage than Central and South Asian genomes (tables S6 and S7). One possible explanation for reduced archaic coverage is a population bottleneck after admixture, which would also lead to increased homozygosity of archaic tracts. In support of this, we found both elevated homozygosity of archaic tracts and 2.3 to 3.4% less archaic coverage than expected given per-individual levels of introgression in five Oceanic groups with bottleneck signals (Baining-Kagat, Baining-Mali, Ata, Mamusi, and Bellona/Rennell) (Fig. 2D and figs. S53 to S55).

In addition to being more geographically restricted relative to Neanderthal introgression, Denisovan introgression likely occurred in multiple pulses from multiple distinct Denisovan-like groups (*12*, *19*, *21*). To analyze the number of putative introgression pulses from Denisovan-like lineages into populations in our dataset, we fit mixture models of between one and six beta-distributed components to the Denisovan match rates of tracts from each population. We recapitulated previous findings of introgression from two Denisovan-like groups in East Asians (figs. S56 to S60 and table S10) and found evidence for introgression from three distinct Denisovan-like groups with differing genetic affinity to the Altai Denisovan into almost all sampled Oceanic populations (Fig. 2E, figs. S61 and S62, and table S10).

Although further work is needed to elucidate the mode, tempo, and landscape of Denisovan introgression, we show that these signals are more widespread than previously thought (*12*, *19*), highlighting the complex dynamics of Denisovan admixture with modern humans.

Natural selection and archaic introgression

Although much of the sequence introgressed from archaic hominins into modern humans is thought to be deleterious or selectively neutral, some genomic regions underwent positive selection after introgression (*29*), a phenomenon known as adaptive introgression. We combined genome-wide scans for positive selection with high-frequency introgressed haplotypes to identify putative adaptive introgressed loci in Oceanic populations (figs. S63 to S67) (*13*). These include previously unidentified candidates linked to skeletal development (*TRPS1*, *BARX1*, *TNC*, *PLK2*), metabolism (*ACAD9*, *DNAJC19*, *CAPSL*, *TBC1D4*, *AGA*, *B4GALNT3*, *ADO*), fertility and reproduction (*HFM1*), and immunity (*FIBCD1*, *ANXA1*, *EGR2*, *FBXO15*), as well as known strong Oceanic adaptive introgression candidates at *TNFAIP3* (*12*, *28*, *29*), the *GBP* cluster (*5*, *30*, *31*), *CD33* (*12*), *CUBN* (*12*, *23*), and *SUMF1* (*12*, *19*, *31*, *32*) (figs. S68 to S75 and tables S11 to S14) (*13*).

One of these putatively adaptive introgressed loci was downstream of the *TRPS1* gene (Fig. 3A and figs. S68 and S69) found exclusively in Oceania and Island Southeast Asia, with frequencies approaching 75% in the Baining groups and Bellona/Rennell (Fig. 3B). *TRPS1* is a transcriptional repressor involved in bone development, craniofacial morphology (*33*, *34*), skeletal defects, hair loss, and the eponymous tricho-rhino-phalangeal syndrome (*35*). To our knowledge, this is the first evidence for adaptive introgression of *TRPS1* into Oceanic populations. While the Neanderthal and Denisovan haplotypes show substantial similarity at this locus, haplotype network analysis indicated that the predominant Oceanic haplogroup is of Denisovan origin (Fig. 3C and figs. S76 and S77). Previous work has identified selection on *TRPS1* in both central African rainforest hunter-gatherer groups and highland Ecuadorians (*36*, *37*) as well as introgression from a superarchaic group into present-day Africans (*38*), suggesting parallel local adaptations at *TRPS1* in response to environmental pressures at the Equator.

Functional characterization of archaic introgressed variants

To understand the phenotypic impacts of archaic introgressed variants, we first annotated archaic introgressed SNVs identified by Sprime for protein-coding and splicing consequences. Among the 713,740 unique introgressed SNVs found in Oceanic groups (table S15), 33,355 were found on high-frequency haplotypes, referred to hereafter as "high frequency archaic SNVs" (hfaSNVs). Of these, 998 (3.0%) hfaSNVs

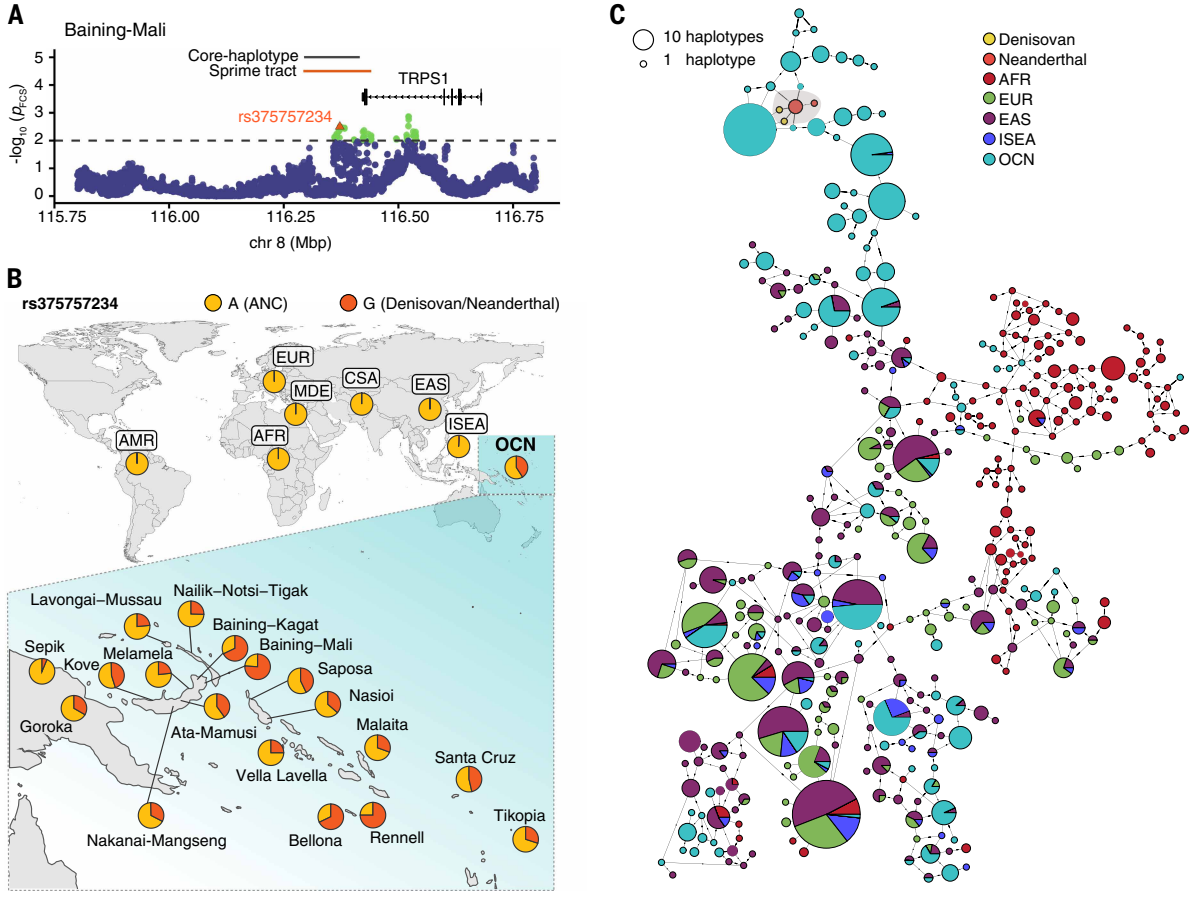

Fig. 3. Novel adaptive introgressed region at the *TRPS1* locus. (**A**) Local Manhattan plot of the *TRPS1* locus showing the $-\log_{10}$ of the Fisher's combined score *P* value (p_{FCS}) in the Baining-Mali population. The Baining-Mali Sprime tract and high-frequency archaic core haplotype are annotated as orange and black bars, respectively. The archaic SNV nearest the peak adaptive introgression signal (rs375757234) is shown as an orange triangle. (**B**) Allele frequencies at rs375757234 in worldwide regions (top) and Oceanic populations (bottom). "A" is the ancestral (shown in yellow), and "G" is the derived archaic allele (shown in orange). (**C**) A minimum spanning network of haplotypes along the Baining-Mali Sprime tract at the *TRPS1* locus (chr8:116292869-116440667). Haplotypes from the Altai Denisovan (yellow), all three Neanderthals (red), and modern humans from Oceania, Island Southeast Asia, East Asia, Europe, and Africa are included. The subgraph containing archaic haplotypes is highlighted in gray. Node area is proportional to the number of chromosomes with that haplotype, and pie charts represent nodes found in multiple geographic regions. Ticks on edges represent mutations between haplotypes.

localized to exonic and splicing regions, including 167 missense, 10 LoF mutations (Fig. 4A), and 60 additional SNVs predicted to be splice-disrupting (table S16) (*13*). These affect 129, 10, and 54 genes respectively (179 total unique genes). Overall, we found an enrichment of hfaSNVs in exonic/splicing regions relative to all introgressed SNVs (OR = 1.26, $P = 1.9 \times 10^{-11}$, Fisher's exact test; fig. S78) but a depletion of missense, LoF, and splice-disrupting hfaSNVs relative to synonymous mutations (OR = 0.73, $P = 0.0012$). This suggests that although adaptive introgression is enriched near genes, it may be driven by mutations that do not affect protein coding or transcript splicing.

We then considered potential noncoding regulatory effects of hfaSNVs, as the vast majority (97%) are intronic or intergenic. We annotated introgressed SNVs overlapping candidate cis-regulatory elements (cCREs), DNaseI hypersensitive sites (DHSs), and enhancer catalogs (*13*). We found an enrichment of hfaSNVs in cCREs relative to all introgressed SNVs (OR = 1.30, $P = 6.5 \times 10^{-94}$), with 66% of hfaSNVs falling in distal enhancers, 10% in proximal enhancers, and 2% in promoters (Fig. 4A). Furthermore, we found significant enrichments of hfaSNVs in immune-related DHSs and enhancers (lymphoid: OR = 1.19, $P = 8.37 \times 10^{-6}$; T cell: OR = 1.24, $P = 5.77 \times 10^{-12}$; B cell: OR = 1.19, $P = 3.51 \times 10^{-10}$; thymus: OR = 1.22, $P = 1.44 \times 10^{-8}$; Fig. 4B) that were consistent across Oceanic populations and archaic origins (figs. S79 and S80), underscoring the major role of adaptive introgression in immune response (*29*, *39*). Conversely, we observed a significant depletion of hfaSNVs in neural DHSs (OR = 0.91, $P = 0.0012$; Fig. 4B), suggesting that purifying selection has occurred against brain-related introgressed variation (*29*, *39*).

We then interrogated potential trait and clinical phenotype associations of hfaSNVs on the basis of overlap with variants from multiple biobanks (*13*). Only 406 (1.2%) hfaSNVs were found in ClinVar, all of which were Benign/Likely Benign or Variants of Uncertain Significance, while 51 (0.15%) hfaSNVs matched fine-mapped variants (posterior inclusion probability ≥ 0.1) from the UK Biobank (UKBB) and BioBank Japan (BBJ) (tables S17 and S18). Of these, far fewer Denisovan hfaSNVs (65 ClinVar, 2 UKBB+BBJ) were found than Neanderthal hfaSNVs (289 ClinVar, 47 UKBB+BBJ), underscoring the large amount of population-specific variation found in Oceania absent from existing biobanks (*40*). Overlaps included Denisovan hfaSNVs associated with glomerular filtration rate and balding and Neanderthal hfaSNVs associated with white blood cell count, albumin/globulin ratio, and adult height (table S18).

While these clinical and biobank-based annotations revealed some putative phenotypically and clinically relevant variants, the functional consequences of the vast majority of Oceania-specific archaic variants remain uncertain. To identify functional, putatively causal adaptive alleles underlying the enrichment of immune-related regulatory elements in adaptive introgressed loci (Fig. 4B), we deployed a massively parallel reporter assay (MPRA) in relevant immune cell lines (*41*). In brief, an MPRA consists of integrating genetic variants of interest, their flanking sequence, and a variant-specific barcode into a vector containing a reporter gene, then transfecting the resulting library of vectors into a cell line. Variants whose alleles alter expression of the reporter gene can then be detected with bulk RNA sequencing of these cells. We tested a pilot dataset of 22,313 hfaSNVs for their effects on gene expression in K562 (lymphoblast) and Jurkat (T lymphocyte) cells (Fig. 4C and tables S19 and S20) (*13*). These MPRAs were highly consistent across replicates (correlation coefficient ≥ 0.95; figs. S81 and S82), recapitulated regulatory effects at known loci (fig. S83, A and B), and displayed biologically relevant CRE activity in tested immune cell types (figs. S83, C and D, and S84A). Overall, we identified 3127 significant expression-modulating variants (emVars) in any cell type (fig. S83, E to G, and table S21). These emVars recapitulated orthogonal measures of CRE activity such as enrichment in DHSs, transcription factor (TF) motif disruption, TF chromatin immunoprecipitation sequencing (ChIP-seq) peaks, and DNase TF footprints (fig. S84, B to E) and preferentially disrupted immune-related TF motifs ($P = 4.2 \times 10^{-8}$, *t* test; figs. S85 and S86).

As most high-frequency introgressed emVars were found in distal enhancers (66.4%, 2077), we next sought to link emVars to their target genes using gene-enhancer linkage maps (*13*). We linked 1551 high-frequency introgressed emVars to 1422 candidate target genes ("gene-linked emVars"), with some having as many as 10 gene-linked emVars (fig. S87A and table S22). Among these was *TNFAIP3*, a known candidate of Denisovan introgression in Oceania (figs. S88 and S89) that serves as an important negative regulator of innate and adaptive immunity (*5*, *12*, *13*, *19*, *23*, *30*–*32*). The Denisovan *TNFAIP3* haplotype carries two missense variants conferring greater immunity without increased autoimmune risk (*42*), and we identified an additional six gene-linked emVars, three of which are predicted to disrupt immune-related TF motifs (STAT4, EGR2, and PPARA; Fig. 4D).

One group of emVar targets included three known adaptive introgression candidates involved in the interferon gamma (IFN-γ) and alpha/beta (IFN-α/β) signaling pathways: *OAS1* (*12*, *43*, *44*), *GBP2* (*5*, *30*), and *JAK1* (*12*, *45*). Although much work has focused on the COVID-19 protective Neanderthal *OAS1* haplotype found in Europeans and East Asians (*29*, *46*, *47*), we found a Denisovan haplotype in Oceania with three missense variants and an intronic variant, all of which were gene-linked emVars (Fig. 4E and figs. S90 and S91), including two previously identified emVars (rs146859513 and rs143462183) (*44*). In *GBP2*, we identified six gene-linked emVars, four of which overlapped T and B cell enhancers, including one synonymous variant predicted to disrupt binding of the lymphoid TF ELF1 (Fig. 4F), highlighting the importance of noncoding regulatory function even for exonic regions (*48*). The GBP haplotype presents a curious evolutionary case, as the two major haplogroups in present-day humans also segregated in Neanderthals, and the introgressed haplotype is also found in the Altai Denisovan (figs. S92 and S93), suggesting the possibility of long-term balancing selection. In *JAK1*, we identified seven gene-linked emVars on a Denisovan haplotype, including a cluster of three expression-increasing emVars overlapping a single T/B cell enhancer ~44 thousand base pairs upstream of *JAK1* (Fig. 4G and fig. S94) that the nearest gene approach incorrectly associates with the nearby *LINC01359*, highlighting the importance of integrating gene-enhancer maps.

Finally, we looked for gene set enrichment of all genes linked to putatively functional hfaSNVs (coding, splice-disrupting, and noncoding emVars) (fig. S87B and table S16). We found significant enrichment [false discovery rate (FDR) < 0.01, Fisher's exact test] of genes with functional variants (especially noncoding) involved in IFN-γ signaling, immune system signaling, and development (Fig. 5A and table S23). For IFN-γ signaling, there were signals of adaptive introgression at 8 of 11 genes with functional variants, spanning Oceanic populations and all three archaic origins, further supporting the role of the IFN-γ signaling pathway in local adaptation in Oceania (Fig. 5B). These genes encompassed a variety of functions, including core IFN-γ genes (*IFNGR1* and *JAK1*), regulation of the signaling cascade (*CAMK2A* and *PIAS1*), and downstream antiviral and immunoregulatory genes (*OAS1*, *GBP2/7/4/6*, *HLA-DRA*, and *TRIM10*). Additional known and novel signals of adaptive introgression were found in the IFN-α/β pathway (*STAT2*, *MX2*) (Fig. 5C) (*49*).

Malaria has long been present in Near Oceania, and an argument has been made that malaria was the "most important determinant of pre-colonial population distribution in [Papua New Guinea]" (*50*). Incidentally, *Plasmodium falciparum*, the most common cause of malaria in Papua New Guinea, is known to trigger IFN-γ secretion at multiple stages of infection (*51*). Of the 97 loci associated with malaria susceptibility in a recent study (*52*), two (rs9268560 and rs572459786) overlapped adaptive introgression candidate regions at genes in the IFN-γ signaling pathway (*HLA-DRA* and *TNFAIP3*). Our analyses indicate that selection acted on archaic introgressed variants at multiple distinct members of the IFN-γ signaling pathway in different Oceanic

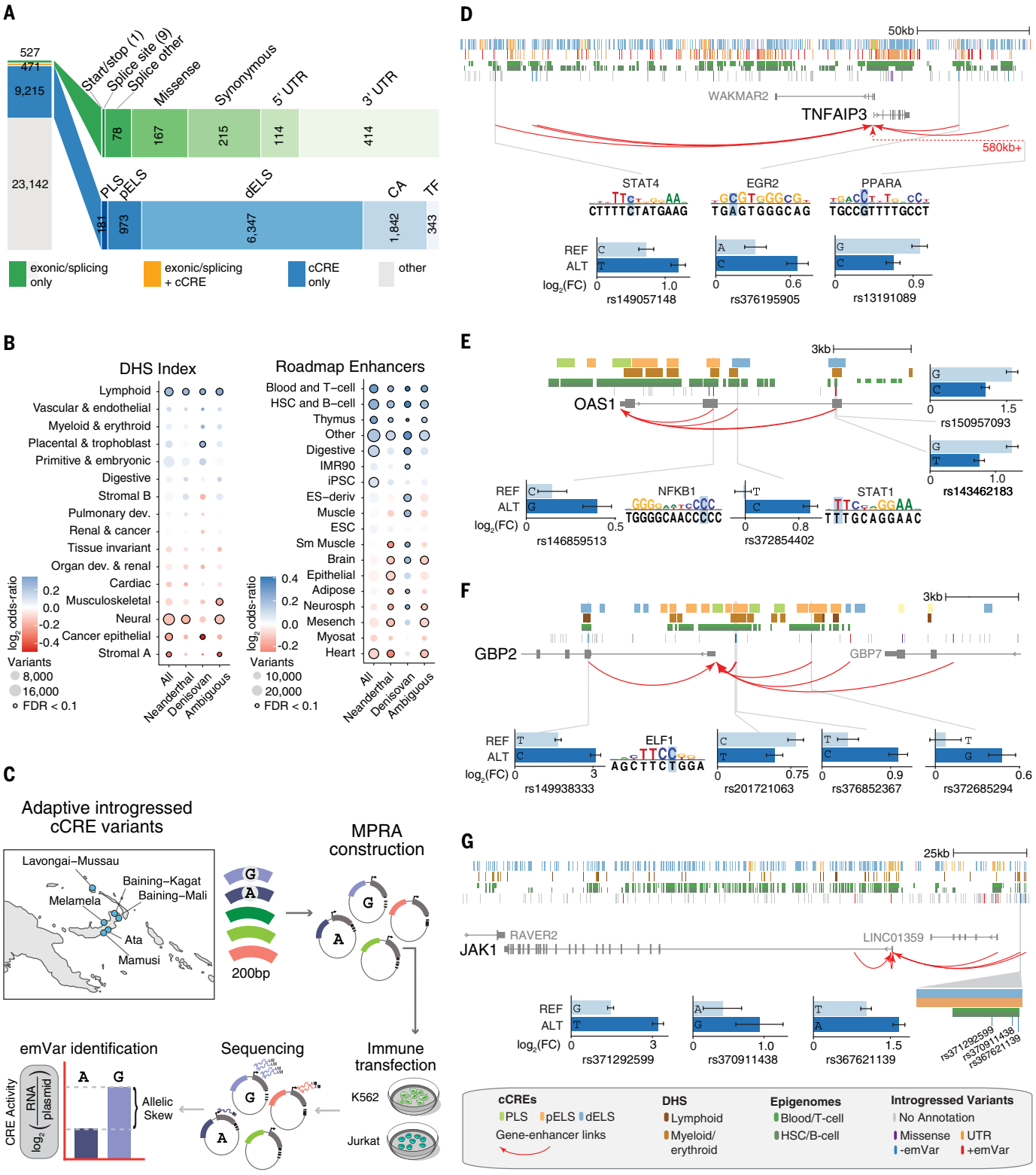

Fig. 4. Functional annotations, enrichments, and MPRAs of hfaSNVs. (**A**) Distribution of exonic and splicing consequences of Near Oceanic hfaSNVs based on Ensembl VEP and overlap with ENCODE CRE annotations. Start/stop, start codon lost or stop codon gained or lost; splice site, acceptor and donor variants; splice other, other splicing effects; UTR, untranslated regions; PLS, promoter-like signature; pELS, proximal enhancer-like signature; dELS, distal enhancer-like signature; TF, transcription factor binding site; CA, chromatin accessible. (**B**) Enrichments of DNase I hypersensitive site (DHS) vocabulary terms from DHS Index and enhancer region catalogs from Roadmap Epigenomics for hfaSNVs relative to all introgressed SNVs, highlighted if FDR < 0.1 (black circles, *P* values from Fisher's exact test). (**C**) Overview of MPRA of high-frequency introgressed SNVs in immune cell lines to assess regulatory activity and identify emVars with allelic differences in RNA/DNA ratios. (**D** to **G**) Discovered emVars overlapping ENCODE CRE annotations, DHS Index vocabulary terms, Roadmap Epigenomics enhancer catalogs, and predicted gene-enhancer links from ABC, EpiMap, and Roadmap Epigenomics for immune genes *TNFAIP3*, *OAS1*, *GBP2*, and *JAK1*. Bar plots show MPRA activity of reference and alternate alleles [$\log_2$ fold change (FC)]. Motifs show predicted immune-related TF motif disruptions.

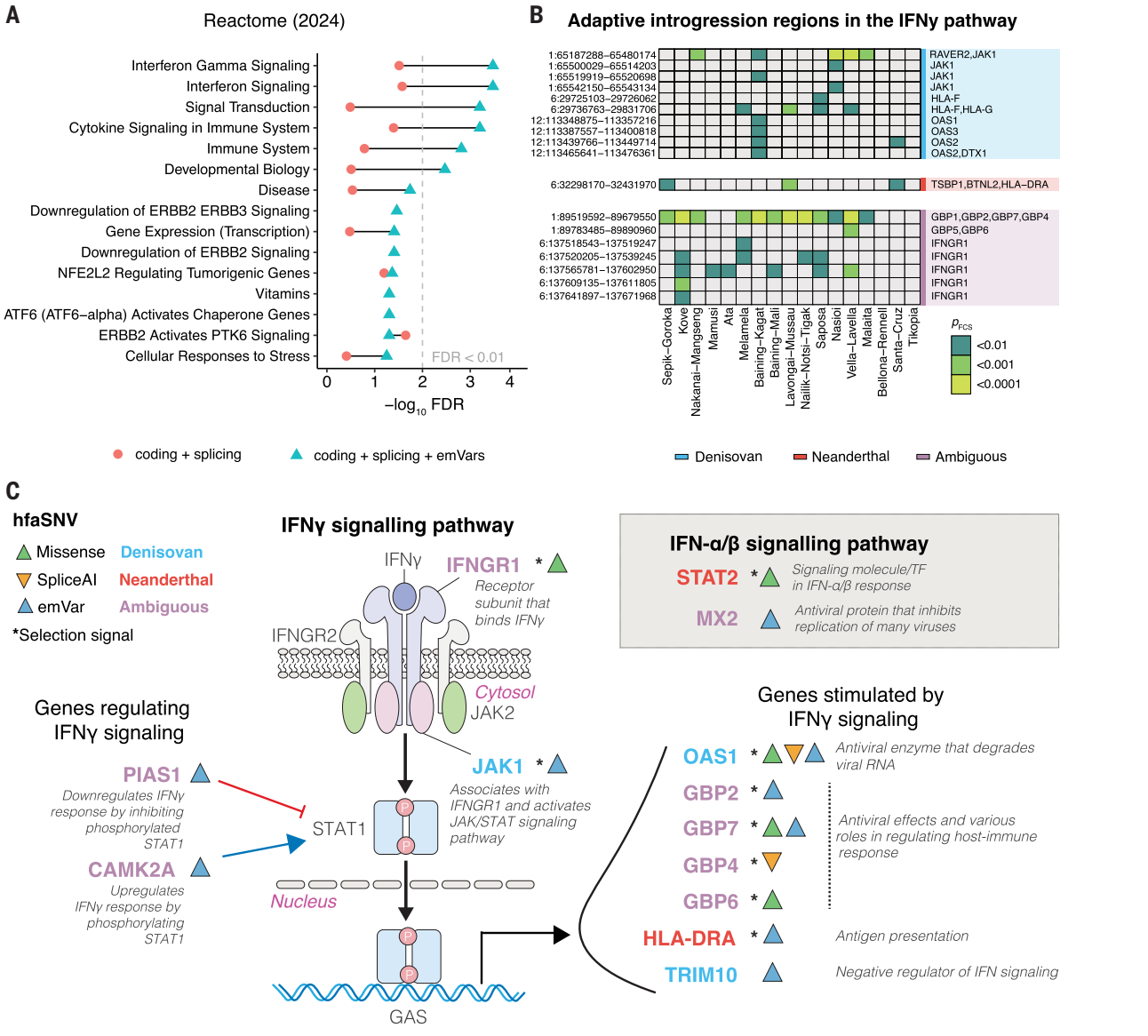

Fig. 5. Adaptive introgressed regions related to the IFN-γ pathway. (**A**) Enriched Reactome pathways (top 15) from Enrichr based on hfaSNVs linked to genes by protein-coding and splice disruption annotations (coding + splicing, red) or also including gene-linked emVars (coding + splicing + emVars, teal). Only gene sets with at least two queried genes are shown. (**B**) Heatmap of adaptive introgression candidate regions of Denisovan, Neanderthal, and ambiguous origin in the IFN-γ signaling pathway. Cells are colored according to the maximum $-\log_{10}$ Fisher's combined score *P* value (p_{FCS}) of windows in the region. Genes overlapping or proximal to each adaptive introgression candidate region involved in the IFN-γ pathway are shown on the right, with background color indicating archaic origin (Denisovan, blue; Neanderthal, red; ambiguous, purple). (**C**) Adaptive introgression candidates in the IFN-γ signaling pathway. Immune genes in the IFN-γ signaling pathway linked to hfaSNVs annotated as missense (green triangle), splice disrupting (orange triangle, SpliceAI ≥ 0.2), or emVars (blue triangle), and classified as Neanderthal (red), Denisovan (blue), or ambiguous (purple) origin. Asterisks indicate loci overlapping adaptive introgression candidate regions. GAS, IFN-γ activation site; red blunt arrow, inhibition; blue sharp arrow, stimulation.

populations (Fig. 5B) rather than on the same pathway members across populations. This is consistent with multiple independent instances of local adaptation in response to novel immune environments and pathogens during human dispersal into the Pacific. Many immune-related genes including novel and known adaptive introgression candidates identified in this study are also pleiotropic (*13*). For example, *TRPS1* plays a role in the differentiation of $CD4^+$ T cells into T helper 17 cells (*53*) in addition to aforementioned roles in bone development and craniofacial morphology (*33*, *34*). We identified three adaptive introgressed emVars downstream of *TRPS1*, including an expression-increasing emVar (rs370787388, T>C) overlapping an active enhancer in hematopoietic stem cells and B cells that is predicted to increase STAT1::STAT2 binding, and a pair of expression-increasing (rs369973466, G>A) and expression-decreasing (rs377623526, G>T) emVars overlapping active enhancers in brain, digestive, epithelial, embryonic stem cell, and heart tissues (figs. S77 and S95A). In addition, the known Neanderthal adaptive introgression candidate *TANK* (*12*, *45*) both suppresses constitutive inflammatory signals from commensal microflora in the intestine (*54*) and is involved in osteoclastogenesis (*55*). We identified three gene-linked emVars, including two intronic expression-increasing emVars, one of which (rs62575578, C>G) overlapped a lymphoid DHS region, and the other (rs28365919, G>A) overlapped an ubiquitous enhancer and is predicted to disrupt binding of the osteogenesis-related TF RUNX2 (fig. S95B). While selective pressures on the immune system were pervasive

throughout human evolutionary history (*56*), the early settlers of Near Oceania were likely small groups that faced resource-poor island environments (*16*), introducing additional selective pressures. Thus, the adaptations we observed at pleiotropic immune-related genes may have arisen as a consequence of these other selective pressures or even antagonistic pleiotropy between immune and other constraints. To tease apart the environmental drivers of these adaptations and better understand the consequences to present-day Near Oceanians, further work will be necessary, including precision genome engineering of archaic introgressed variants and haplotypes, culturing of organoids with these gene edits, and assays exploring responses to factors such as immune stimuli and nutrient limitations.

These islands, at the edge of human habitation for tens of thousands of years, are home to populations with remarkable genetic variation shaped by their isolation, resultant bottlenecks, local adaptations, and selection on archaic introgressed variants. The latter was greatly facilitated by the substantial amounts of archaic introgressed sequence uniquely harbored by Near Oceanic populations, including the largest amount of Denisovan sequence worldwide. In the largest study of Denisovan introgressed variation to date, we characterized the functional consequences of archaic introgressed variants found at high frequency in Near Oceanians and identified putatively causal archaic variants contributing to parallel local adaptation of both the immune system and skeletal development.

Materials and methods are available in the supplementary materials.

REFERENCES AND NOTES

1. A. Pawley, R. Green, Dating the dispersal of the oceanic languages. *Ocean. Linguist.* **12**, 1–67 (1973). doi: 10.2307/3622852
2. G. Kerby, A. Ford, G. R. Summerhayes, M. G. Leavesley, J. M. Palin, Fit for purpose: Investigating adaptations in late Pleistocene lithic technology to an island environment at Buang Merabak, New Ireland, Papua New Guinea. *World Archaeol.* **54**, 317–337 (2022). doi: 10.1080/00438243.2023.2172070
3. J. S. Friedlaender *et al.*, The genetic structure of Pacific Islanders. *PLOS Genet.* **4**, e19 (2008). doi: 10.1371/journal.pgen.0040019; pmid: 18208337
4. J. S. Friedlaender, W. W. Howells, J. G. Rhoads, Eds., *The Solomon Islands Project: A Long-Term Study of Health, Human Biology, and Culture Change*, vol. 4 of *Research Monographs on Human Population Biology* (Clarendon Press, 1987).
5. B. Vernot *et al.*, Excavating Neandertal and Denisovan DNA from the genomes of Melanesian individuals. *Science* **352**, 235–239 (2016). doi: 10.1126/science.aad9416; pmid: 26989198
6. A. Bergström *et al.*, Insights into human genetic variation and population history from 929 diverse genomes. *Science* **367**, eaay5012 (2020). doi: 10.1126/science.aay5012; pmid: 32193295
7. 1000 Genomes Project Consortium, A global reference for human genetic variation. *Nature* **526**, 68–74 (2015). doi: 10.1038/nature15393; pmid: 26432245
8. GTEx Consortium, The GTEx Consortium atlas of genetic regulatory effects across human tissues. *Science* **369**, 1318–1330 (2020). doi: 10.1126/science.aaz1776; pmid: 32913098
9. S. Chen *et al.*, A genomic mutational constraint map using variation in 76,156 human genomes. *Nature* **625**, 92–100 (2024). doi: 10.1038/s41586-023-06045-0; pmid: 38057664
10. S. Mallick *et al.*, The Simons Genome Diversity Project: 300 genomes from 142 d iverse populations. *Nature* **538**, 201–206 (2016). doi: 10.1038/nature18964; pmid: 27654912
11. S. Tucci *et al.*, Evolutionary history and adaptation of a human pygmy population of Flores Island, Indonesia. *Science* **361**, 511–516 (2018). doi: 10.1126/science.aar8486; pmid: 30072539
12. J. Choin *et al.*, Genomic insights into population history and biological adaptation in Oceania. *Nature* **592**, 583–589 (2021). doi: 10.1038/s41586-021-03236-5; pmid: 33854233
13. See supplementary materials.
14. Although the Mamusi currently speak an Austronesian/Oceanic language, it is thought that this arose through a language replacement event and that they originally spoke a Papuan language (*3*).
15. A. M.-S. Ko *et al.*, Early Austronesians: Into and out of Taiwan. *Am. J. Hum. Genet.* **94**, 426–436 (2014). doi: 10.1016/j.ajhg.2014.02.003; pmid: 24607387
16. G. Summerhayes, "The archaeology of Melanesia" in *The Melanesian World* , E. Hirsch, W. Rollason, Eds. (Routledge, 2019), pp. 43–62.
17. D. J. Lawson, L. van Dorp, D. Falush, A tutorial on how not to over-interpret STRUCTURE and ADMIXTURE bar plots. *Nat. Commun.* **9**, 3258 (2018). doi: 10.1038/s41467-018-05257-7; pmid: 30108219
18. J. Terhorst, J. A. Kamm, Y. S. Song, Robust and scalable inference of population history from hundreds of unphased whole genomes. *Nat. Genet.* **49**, 303–309 (2017). doi: 10.1038/ng.3748; pmid: 28024154
19. G. S. Jacobs *et al.*, Multiple deeply divergent Denisovan ancestries in Papuans. *Cell* **177**, 1010–1021.e32 (2019). doi: 10.1016/j.cell.2019.02.035; pmid: 30981557
20. A. Bergström, C. Stringer, M. Hajdinjak, E. M. L. Scerri, P. Skoglund, Origins of modern human ancestry. *Nature* **590**, 229–237 (2021). doi: 10.1038/s41586-021-03244-5; pmid: 33568824
21. S. R. Browning, B. L. Browning, Y. Zhou, S. Tucci, J. M. Akey, Analysis of human sequence data reveals two pulses of archaic Denisovan admixture. *Cell* **173**, 53–61.e9 (2018). doi: 10.1016/j.cell.2018.02.031; pmid: 29551270
22. L. Skov *et al.*, The nature of Neanderthal introgression revealed by 27,566 Icelandic genomes. *Nature* **582**, 78–83 (2020). doi: 10.1038/s41586-020-2225-9; pmid: 32494067
23. S. Sankararaman, S. Mallick, N. Patterson, D. Reich, The combined landscape of Denisovan and Neanderthal ancestry in present-day humans. *Curr. Biol.* **26**, 1241–1247 (2016). doi: 10.1016/j.cub.2016.03.037; pmid: 27032491
24. G. H. Perry *et al.*, Diet and the evolution of human amylase gene copy number variation. *Nat. Genet.* **39**, 1256–1260 (2007). doi: 10.1038/ng2123; pmid: 17828263
25. C. E. Inchley *et al.*, Selective sweep on human amylase genes postdates the split with Neanderthals. *Sci. Rep.* **6**, 37198 (2016). doi: 10.1038/srep37198; pmid: 27853181
26. P. Qin, M. Stoneking, Denisovan ancestry in East Eurasian and Native American populations. *Mol. Biol. Evol.* **32**, 2665–2674 (2015). doi: 10.1093/molbev/msv141; pmid: 26104010
27. A.-S. Malaspinas *et al.*, A genomic history of Aboriginal Australia. *Nature* **538**, 207–214 (2016). doi: 10.1038/nature18299; pmid: 27654914
28. K. E. Witt, F. Villanea, E. Loughran, X. Zhang, E. Huerta-Sanchez, Apportioning archaic variants among modern populations. *Philos. Trans. R. Soc. Lond. B Biol. Sci.* **377**, 20200411 (2022). doi: 10.1098/rstb.2020.0411; pmid: 35430882
29. P. F. Reilly, A. Tjahjadi, S. L. Miller, J. M. Akey, S. Tucci, The contribution of Neanderthal introgression to modern human traits. *Curr. Biol.* **32**, R970–R983 (2022). doi: 10.1016/j.cub.2022.08.027; pmid: 36167050
30. R. M. Gittelman *et al.*, Archaic Hominin admixture facilitated adaptation to out-of-Africa environments. *Curr. Biol.* **26**, 3375–3382 (2016). doi: 10.1016/j.cub.2016.10.041; pmid: 27839976
31. N. Brucato *et al.*, Chronology of natural selection in Oceanian genomes. *iScience* **25**, 104583 (2022). doi: 10.1016/j.isci.2022.104583; pmid: 35880026
32. G. Gower, P. I. Picazo, M. Fumagalli, F. Racimo, Detecting adaptive introgression in human evolution using convolutional neural networks. *eLife* **10**, e64669 (2021). doi: 10.7554/eLife.64669; pmid: 34032215
33. C. L. Ackert-Bicknell *et al.*, Genetic variation in *TRPS1* may regulate hip geometry as well as bone mineral density. *Bone* **50**, 1188–1195 (2012). doi: 10.1016/j.bone.2012.01.011; pmid: 22306695
34. I. Michikami *et al.*, Trps1 is necessary for normal temporomandibular joint development. *Cell Tissue Res.* **348**, 131–140 (2012). doi: 10.1007/s00441-012-1372-1; pmid: 22427063
35. T. H. Malik, D. Von Stechow, R. T. Bronson, R. A. Shivdasani, Deletion of the GATA domain of TRPS1 causes an absence of facial hair and provides new insights into the bone disorder in inherited tricho-rhino-phalangeal syndromes. *Mol. Cell. Biol.* **22**, 8592–8600 (2002). doi: 10.1128/MCB.22.24.8592-8600.2002; pmid: 12446778
36. M. Lopez *et al.*, Genomic evidence for local adaptation of hunter-gatherers to the African rainforest. *Curr. Biol.* **29**, 2926–2935.e4 (2019). doi: 10.1016/j.cub.2019.07.013; pmid: 31402299
37. S. K. Joseph *et al.*, Genomic evidence for adaptation to tuberculosis in the Andes before European contact. *iScience* **26**, 106034 (2023). doi: 10.1016/j.isci.2023.106034; pmid: 36824277
38. A. Durvasula, S. Sankararaman, Recovering signals of ghost archaic introgression in African populations. *Sci. Adv.* **6**, eaax5097 (2020). doi: 10.1126/sciadv.aax5097; pmid: 32095519
39. K. D. Ahlquist *et al.*, Our tangled family tree: New genomic methods offer insight into the legacy of archaic admixture. *Genome Biol. Evol.* **13**, evab115 (2021). doi: 10.1093/gbe/evab115; pmid: 34028527
40. M. C. Mills, C. Rahal, The GWAS Diversity Monitor tracks diversity by disease in real time. *Nat. Genet.* **52**, 242–243 (2020). doi: 10.1038/s41588-020-0580-y; pmid: 32139905
41. R. Tewhey *et al.*, Direct identification of hundreds of expression-modulating variants using a multiplexed reporter assay. *Cell* **165**, 1519–1529 (2016). doi: 10.1016/j.cell.2016.04.027; pmid: 27259153
42. N. W. Zammit *et al.*, Denisovan, modern human and mouse *TNFAIP3* alleles tune A20 phosphorylation and immunity. *Nat. Immunol.* **20**, 1299–1310 (2019). doi: 10.1038/s41590-019-0492-0; pmid: 31534238
43. F. L. Mendez, J. C. Watkins, M. F. Hammer, Global genetic variation at *OAS1* provides evidence of archaic admixture in Melanesian populations. *Mol. Biol. Evol.* **29**, 1513–1520 (2012). doi: 10.1093/molbev/msr301; pmid: 22319157
44. D. M. Vespasiani *et al.*, Denisovan introgression has shaped the immune system of present-day Papuans. *PLOS Genet.* **18**, e1010470 (2022). doi: 10.1371/journal.pgen.1010470; pmid: 36480515
45. A. Gouy, L. Excoffier, Polygenic patterns of adaptive introgression in modern humans are mainly shaped by response to pathogens. *Mol. Biol. Evol.* **37**, 1420–1433 (2020). doi: 10.1093/molbev/msz306; pmid: 31935281

46. E. Jagoda *et al.*, Detection of Neanderthal adaptively introgressed genetic variants that modulate reporter gene expression in human immune cells. *Mol. Biol. Evol.* **39**, msab304 (2022). doi: 10.1093/molbev/msab304; pmid: 34662402
47. E. Jagoda *et al.*, Regulatory dissection of the severe COVID-19 risk locus introgressed by Neanderthals. *eLife* **12**, e71235 (2023). doi: 10.7554/eLife.71235; pmid: 36763080
48. N. Ahituv, Exonic enhancers: Proceed with caution in exome and genome sequencing studies. *Genome Med.* **8**, 14 (2016). doi: 10.1186/s13073-016-0277-0; pmid: 26856702
49. F. L. Mendez, J. C. Watkins, M. F. Hammer, A haplotype at *STAT2* introgressed from Neanderthals and serves as a candidate of positive selection in Papua New Guinea. *Am. J. Hum. Genet.* **91**, 265–274 (2012). doi: 10.1016/j.ajhg.2012.06.015; pmid: 22883142
50. R. Attenborough, G. Jacobs, P. Kusuma, "Deep histories in New Guinea: Insights from genetics on human adaptation to malaria and diverse environments" in *West New Guinea: Social, Biological, and Material Histories*, D. Gaffney, M. Tolla, Eds., vol. 58 of *Terra Australis* (ANU Press, ed. 1, 2025), pp. 119–146.
51. E. B. Belachew, Immune response and evasion mechanisms of *Plasmodium falciparum* parasites. *J. Immunol. Res.* **2018**, 6529681 (2018). doi: 10.1155/2018/6529681; pmid: 29765991
52. Malaria Genomic Epidemiology Network, Insights into malaria susceptibility using genome-wide data on 17,000 individuals from Africa, Asia and Oceania. *Nat. Commun.* **10**, 5732 (2019). doi: 10.1038/s41467-019-13480-z; pmid: 31844061
53. N. Yosef *et al.*, Dynamic regulatory network controlling T_H17 cell differentiation. *Nature* **496**, 461–468 (2013). doi: 10.1038/nature11981; pmid: 23467089
54. T. Kawagoe *et al.*, TANK is a negative regulator of Toll-like receptor signaling and is critical for the prevention of autoimmune nephritis. *Nat. Immunol.* **10**, 965–972 (2009). doi: 10.1038/ni.1771; pmid: 19668221
55. K. Maruyama, T. Kawagoe, T. Kondo, S. Akira, O. Takeuchi, TRAF family member-associated NF-κB activator (TANK) is a negative regulator of osteoclastogenesis and bone formation. *J. Biol. Chem.* **287**, 29114–29124 (2012). doi: 10.1074/jbc.M112.347799; pmid: 22773835
56. L. B. Barreiro, L. Quintana-Murci, From evolutionary genetics to human immunology: How selection shapes host defence genes. *Nat. Rev. Genet.* **11**, 17–30 (2010). doi: 10.1038/nrg2698; pmid: 19953080
57. S. Tucci, Supplemental data from: Long-term isolation and archaic introgression shape functional genetic variation in Near Oceania [Dataset], version 1.0, Dryad (2026); https://doi.org/10.5061/dryad.2fqz612z6.
58. D. Tejada Martinez, S. Rong, C. Liu, A. Tjahjadi, P. F. Reilly, YourePrettyGood/PIBv1_manuscript, version 1.0.1, Zenodo (2026); https://doi.org/10.5281/zenodo.18895142.

ACKNOWLEDGMENTS

We owe a large debt of gratitude to the participants in this study from different parts of Near Oceania who collaborated with us in this project so willingly. We acknowledge D. Hrdy and H. Norton for providing support with field collections in Papua New Guinea. We thank L. Aiello, C. Barbieri, E. Green, A. Manica, R. Polimanti, M. Trizzino, P. Visscher, L. Yengo, and J. Akey for helpful feedback on this work. We also thank A. Tejada Martinez for graphic design support. We are grateful to several anonymous reviewers for their helpful feedback. We dedicate this work to Françoise R. Friedlaender, an inspiring woman in STEM and our dear friend. **Funding:** Research reported in this publication was supported by the National Institute of General Medical Sciences and the National Human Genome Research Institute of the National Institutes of Health under award numbers R35GM147565 (to S.T.), R00HG010669 (to S.K.R.), R01HG012872 (to S.K.R.), and 1S10OD030363-01A1. Research reported in this publication was supported, in part, by the Theresa Seessel Fund and the Biological Sciences Fund of Yale University to S.T. and P.F.R. The content is solely the responsibility of the authors and does not necessarily represent the official views of the National Institutes of Health. **Author contributions:** S.T. and J.S.F. conceived the project. J.S.F., G.K., and D.A.M. carried out the sample collection. S.T. and S.K.R. supervised analysis. P.F.R., F.R.F., and J.S.F. performed the data curation and processing. S.L.M. and A.P. extracted DNA, and S.K.R., S.L.M., J.A., and M.E.P. performed the MPRA experiments. P.F.R., D.T.-M., S.R., A.T., C.L., S.L.M., and J.A. performed analyses. P.F.R., S.T., D.T.-M., A.T., and S.R. designed the figures. P.F.R., S.T., D.T.-M., S.K.R., and S.R. wrote the manuscript with input from all authors. **Competing interests:** All authors declare that they have no competing interests. **Data, code, and materials availability:** Whole-genome sequence data have been deposited into the Database of Genotypes and Phenotypes (dbGaP) under accession number phs004464.v1. Whole-genome sequence data from (*12*) can be accessed at the European Genome-phenome Archive (EGA) under accession number EGAD00001006880. MPRA sequence data have been deposited into the Sequence Read Archive (SRA) under accession number PRJNA1435427. No new materials were generated for this study. Code and data directly used to generate the results, figures, and tables are accessible in Dryad (*57*). Code, including pipelines, can also be accessed in Zenodo (*58*) and Github (https://github.com/YourePrettyGood/PIBv1_manuscript/). **License information:** Copyright © 2026 the authors, some rights reserved; exclusive licensee American Association for the Advancement of Science. No claim to original US government works. https://www.science.org/about/science-licenses-journal-article-reuse

SUPPLEMENTARY MATERIALS

science.org/doi/10.1126/science.adr6749
Materials and Methods; Supplementary Text; Figs. S1 to S95; Tables S1 to S23; References (*59*–*261*); MDAR Reproducibility Checklist

Submitted 16 July 2024; resubmitted 5 May 2025; accepted 19 March 2026
10.1126/science.adr6749

Long-term isolation and archaic introgression shape functional genetic variation in Near Oceania

Patrick F. Reilly, Stephen Rong, Daniela Tejada-Martinez, Samantha L. Miller, Audrey Tjahjadi, Chang Liu, Jared Akers, Alysa Pomer, Margaret E. Prentice, D. Andrew Merriwether, Françoise R. Friedlaender, George Koki, Jonathan S. Friedlaender, Steven K. Reilly, and Serena Tucci

Science **392** (6803), eadr6749. DOI: 10.1126/science.adr6749

Editor's summary

Between 2 and 5% of modern Eurasian genomes are derived from admixture with Neanderthals and Denisovans, with Papua New Guineans bearing the largest fractions. However, Oceanian populations remain underrepresented in genetic studies, resulting in questions about the landscape of archaic introgression, including difficult-to-identify features such as structural variants. Hsieh *et al*. used long-read sequencing to identify archaic-derived structural variants in two Papua New Guinean individuals, finding many unique insertions and deletions, as well as 11 centromeres potentially inherited from archaic hominins. Reilly *et al*. examined whole-genome sequences from 177 Near Oceanian individuals, revealing many potentially adaptively introgressed regions. The authors tested some of these for their gene-regulatory potential using massively parallel reporter assays. Together, these studies give us greater insight into how archaic introgression has shaped these historically underrepresented populations. —Corinne Simonti